Journal of Applied Sciences

ISSN 1812-5654

science alert

ANSInet
an open access publisher
http://ansinet.com

Journal of Applied Sciences 8 (23): 4251-4262, 2008
ISSN 1812-5654

Petrography and Geochemistry Characteristic of Enclaves in the Astaneh Pluton (Sanandaj-Sirjan Zone, Western Iran)

[1]Z. Tahmasbi, [1]M. Khalili, [2]A. Castro and [3]A. Ahmadi-Khalaji
[1]Department of Geology, Faculty of Sciences, University of Isfahan, Isfahan, Iran
[2]Department of Geology, University of Huelva, Huelva, Spain
[3]Department of Geology, Faculty of Sciences, University of Lorestan, Khorram Abad, Iran

Abstract: Microgabbrodiorite, microdiorite and less than microgranodiorite enclaves occur in the Astaneh pluton. These enclaves have I-type mineral assemblages that are broadly similar to those in the host granitoids except for the greater abundance of mafic minerals, such as amphibole. They show various features formed by magma mixing/mingling environment: abundant subrounded shape, sharp but partly diffuse contact with host granitoids, finer grain size than host granites, more mafic small enclave in large enclave, ocellar quartz, acicular apatite, poikilitic textures and pargasitic amphibole in dacitic enclave. Indeed geochemistry evidences and enclaves normalized against their host granodiorites show that magma mingling occurred.

Key words: Magma mixing, magma mingling, Sanandaj-Sirjan zone

INTRODUCTION

The study of enclaves is important because it can shed light on the mode of emplacement of granitoid magmas, the nature of the country rocks, the dynamics of magma chambers and cooling plutons and the origin and evolution of granitoid magmas (Barbarin and Didier, 1991).

The microgranular enclaves hosted in granitoids may serve as a potential tool to understand the process of mafic and felsic magma interaction, where microgranular enclaves can represent pristine mafic magma or a hybrid (mafic and felsic) product mingled in convective, calc-alkaline plutonic systems (Castro *et al*., 1990; Wiebe *et al*., 1997). The typical igneous texture described by Vernon (1991) and fine-grained margins surrounding many MME (Mafic Microgranular Enclaves) favor their formation from the crystallization of magma.

The three main theories for the petrogenesis of microgranular enclaves interpret them as: 1 fragments of wallrock facies closely related to the host magma or of cognate fragments of cumulates; 2 globules of more mafic magma, generally hybrid magma, comingled with more felsic host magma and 3 fragments of recrystallized, refractory metamorphic rocks and fragments of melt residues from the granite source as summarized by Maas *et al*. (1997). So clearly the origin of microgranular enclaves is still debated; the most popular choice is the magma mixing and mingling models. Magma mixing causes homogenization of the interacting melt phases and the conversion of early crystals to partly dissolved (corroded) in new hybrid magma, whereas, mingling or co-mingling involves partial mixing or interpenetration of felsic–mafic magmas without pervasive changes (Vernon, 1983; Sparks and Marshall, 1986; Barbarin and Didier, 1992). However, magma mingling (either as cogenetic mafic and felsic magmas or as two coeval magmas) as a mechanism for the genesis of MME, which are common in I-type granitoid rocks, have received the most attention from recent researchers (Didier, 1987; Vernon *et al*., 1988; Dodge and Kistler, 1990; Barbarin and Didier, 1991; Castro *et al*., 1991; Fershtater and Borodina, 1991; Tobisch *et al*., 1997; Sinha *et al*., 2001; Dahlquist, 2002). We will employ the term "mixing when homogenous hybrid rocks are formed and the term mingling or Co-mingling according to Vernon (1990) and Barbarin and Didier (1992), should be restricted to systems with only mechanical interactions. The term hybridization will refer to compositional modifications of the two magmas.

This study presents the mineralogy, petrography, major and trace element geochemistry of microgranular enclaves from the Astaneh area, Sanandaj-Sirjan Zone, Western Iran (Fig. 1). The geochemical data are used to test specific magmatic processes which may have been involved in the genesis of the microgranular enclaves.

MATERIALS AND METHODS

A total of about 50 samples from different enclaves including gabbro dared, dared, tonalite and granodiorite collected. Fifty thin sections of these samples were prepared and studied by optical microscope and 5 thin polished sections were selected for electron microprobe.

Corresponding Author: Zahra Tahmasbi, Department of Geology, Faculty of Sciences, University of Isfahan, Isfahan, Iran Tel: +989163692179 Fax: +983117932159

Representative samples (11 samples) were then selected for whole rock geochemistry. Sample weights were 1-1.5 kg before crushing and powdering. Major, minor and trace element abundances were determined by X-Ray Fluorescence (XRF), using a Borker S4 Pioneer Spectrometer and Inductively Coupled Plasma-Mass Spectrometry (ICP-MS) at the University of Huelva in March 2006 during 6 months, Spain. XRF analysis used approximately 0.1 g rock powder that was first mixed with 0.9 g $Li_2B_4O_7$ in a crucible and then melted in 1150°C. Trace and REE analysis by ICP_MS, in this way used 0.1 g powder that mixed to HF, HCl and HNO_3 in Teflon vials, the analytical processes are described by Cotton *et al.* (1995). Relative standard deviations were ≤ ±2% for major elements and ≤ ±5% for trace elements. The results of the analyses are reported in Table 1. The major element compositions of the minerals were determined by Electron Microprobe analysis of

Table 1: Whole-rock geochemical compositions from the Enclaves and average of host granite of the Astaneh pluton

	Lithology											
	Gabbro dioritic enclaves							Dioritic and granodioritic enclaves				Astaneh granitoid
Sample	EK4	E25	Epa1	CESa4	E10	E17	E19	E38	E28	E29	Ech6	average
SiO_2	52.63	52.63	54.57	54.35	55.74	56.09	57.81	60.49	58.03	59.22	65.41	63.94
TiO_2	0.56	0.56	0.41	0.45	0.53	0.45	0.59	0.74	0.50	0.45	0.44	0.51
Pl_2O_3	15.12	13.98	14.66	14.97	16.73	15.65	17.64	18.25	16.67	16.11	16.67	16.13
Fe_2O_3T	10.52	10.24	10.34	9.06	8.61	7.84	7.70	5.54	8.66	8.94	4.34	5.71
MgO	7.08	7.83	7.28	6.38	5.17	6.33	4.05	2.32	4.55	4.64	2.08	2.71
MnD	0.25	0.23	0.27	0.23	0.19	0.17	0.15	0.93	0.18	0.21	0.06	0.10
CaO	8.95	9.49	8.12	8.53	7.03	8.02	5.66	4.67	6.99	5.86	3.19	4.54
Na_2O	2.67	2.15	2.06	2.52	3.02	2.72	2.60	4.38	2.01	2.35	3.73	2.65
K_2O	1.37	1.32	1.27	1.69	1.69	1.98	2.39	2.41	1.77	1.96	2.68	2.68
P_2O_5	0.09	0.07	0.06	0.06	0.08	0.06	0.09	0.17	0.07	0.07	0.13	0.10
P.F	1.27	0.93	1.44	1.56	1.67	1.70	1.78	0.78	0.97	0.46	1.77	1.35
Total	100.51	100.53	100.61	100.57	100.58	100.70	100.47	99.85	100.40	100.26	100.62	100.47
Li	27.32	25.37	44.15	23.87	46.22	38.66	55.68	31.92	25.34	35.25	30.16	45.28
Be	1.13	1.01	1.40	1.23	1.40	1.10	1.15	1.27	0.81	1.41	1.27	1.48
Sc	29.73	39.60	36.55	46.95	44.13	35.58	22.89	17.98	26.73	33.06	16.35	18.36
V	136.54	172.97	162.20	158.14	139.93	181.66	121.39	107.32	116.76	154.53	67.53	82.67
Cr	304.48	439.70	337.10	370.61	174.58	336.31	96.53	35.39	104.01	165.04	78.31	136.24
Co	25.45	45.38	32.82	27.18	23.81	41.99	16.92	24.61	19.38	24.56	12.73	15.40
Ni	66.84	70.64	88.76	78.95	28.39	41.04	17.88	2.76	17.66	25.17	9.23	15.06
Ou	86.88	50.74	66.20	90.40	63.76	25.71	11.20	87.86	38.61	15.28	145.16	44.05
Zn	67.31	100.89	83.94	90.17	81.05	7.95	65.41	51.84	60.26	72.68	39.14	54.46
Ga	16.36	52.67	19.30	22.25	22.65	51.05	20.27	66.05	18.56	23.37	21.38	26.90
As	11.53	5.15	37.46	4.32	3.80	8.31	7.86	1.95	6.27	7.54	3.08	7.89
Rb	47.01	52.66	60.56	55.03	131.60	60.24	80.01	96.74	49.10	79.51	90.33	90.27
Sr	130.61	155.97	144.07	156.92	147.32	166.36	143.01	254.84	114.26	164.77	175.62	148.09
Y	31.47	31.45	51.49	64.37	28.07	17.22	17.36	15.34	11.61	14.66	14.86	18.29
Zr	31.43	31.34	25.89	10.71	22.32	33.75	82.23	142.86	35.71	37.32	106.43	107.78
Nb	6.76	7.35	7.76	9.18	9.32	6.25	8.37	15.56	5.83	7.16	9.94	9.46
Od	0.21	1.05	0.22	0.14	0.08	0.92	0.08	0.96	0.13	0.13	0.13	0.31
OS	6.86	6.05	8.44	6.51	11.73	4.83	18.31	18.06	5.17	6.22	11.18	11.13
Ba	132.66	261.00	144.09	211.51	219.05	262.00	186.18	298.00	172.52	224.68	219.03	247.94
La	23.05	20.88	20.15	24.73	32.19	16.24	18.44	19.03	12.68	15.39	19.89	22.78
Oe	54.78	47.82	54.35	64.65	60.22	34.37	35.86	34.79	24.27	29.78	37.63	44.24
Pr	8.22	7.28	9.35	11.35	7.58	4.36	4.50	4.17	2.94	3.70	4.71	5.55
Nd	28.19	25.77	36.61	44.11	22.70	14.31	14.89	13.80	9.77	12.21	15.02	18.26
Sm	6.42	6.31	10.18	12.34	4.57	3.02	3.19	2.88	1.91	2.67	3.07	3.73
Eu	0.92	1.06	0.98	1.02	0.74	0.89	0.80	1.06	0.85	0.95	0.80	0.79
Gd	6.12	6.24	10.10	13.02	4.48	2.96	3.20	2.83	2.02	2.51	0.99	3.56
Tb	1.23	1.30	2.14	2.77	0.94	0.56	0.63	0.56	0.40	0.51	0.56	0.68
Dy	6.55	6.48	10.90	14.24	4.95	3.04	3.27	2.81	2.12	2.62	2.83	3.58
Hb	1.53	1.57	2.57	3.38	1.22	0.75	0.83	0.70	0.56	0.65	0.68	0.82
Er	3.87	3.82	6.20	7.99	3.27	1.98	2.06	1.76	1.48	1.79	1.75	2.12
Tm	0.62	0.62	0.99	1.26	0.56	0.32	0.36	0.28	0.26	0.30	0.27	0.34
Yb	3.47	3.30	5.24	6.27	3.15	1.82	2.03	1.52	1.61	1.79	1.55	1.96
Lu	0.58	0.57	0.89	1.06	0.56	0.31	0.35	0.26	0.30	0.33	0.29	0.32
Ta	0.79	1.95	2.02	0.88	1.46	0.61	1.10	1.16	1.56	0.68	1.03	1.40
W	1.44	2.15	2.18	3.48	16.22	3.39	3.58	8.05	4.86	5.70	5.52	7.57
Pb	14.08	32.02	16.29	19.87	13.18	30.47	16.67	21.76	14.36	11.54	10.48	30.06
Th	5.02	3.26	3.67	9.02	20.26	5.74	10.31	7.63	2.92	2.05	9.87	11.01
U	1.22	0.87	2.14	2.02	4.65	1.40	1.94	1.30	0.71	0.70	1.80	0.02
Hf	1.42	2.58	1.81	1.66	1.70	1.85	0.61	1.79	0.77	0.93	0.71	1.34
SumREE	145.55	133.02	170.65	208.19	147.13	84.93	90.41	86.45	61.17	75.20	90.04	108.74
Eu/Eu*	0.451	0.519	0.297	0.247	0.503	0.915	1.33	1.141	1.33	1.13	0.99	0.67
(La/Yb)n	4.44	4.23	2.57	2.64	6.83	5.97	5.27	8.37	5.75	8.58	8.58	7.78

polished thin sections. The analyses were performed with JXA-8200 Super Probe at university of Huelva (Spain), operated with an accelerating voltage 15 keV and a probe current of 5 nA. Silicate standards were Jadeite for Na, wollastonite for Ca, Alkali feldspar for K and Al, enstatite for Mg, fayallite for Fe and Mn and apatite for P.

RESULTS

Geological setting: The Astaneh pluton is a NNW-SSE trending body covering an area of 30 km^2, approximately 10 km in length and 3 km in width, which lies between 33° 30'-34°N and between 49°15'-49°, 25' E (Fig. 1b). b).The Astaneh area is characterized by the predominance of metamorphic rocks of Jurassic age (Baharifar *et al*., 2004) and the presence of the Astaneh pluton. Metamorphic rocks subdivided to 2 groups based on their setting: Dynamothermal and Contact. Dynamotermal metamorphism has affected a vast area and is composed of slate, phyllite and schist (Ahmadi *et al*., 2007). By the injection of the Astaneh pluton, a contact metamorphism has occurred which can be considered as an albite-epidote hornfels facies. Contact metamorphism rocks consist of spotted schist, hornfels schist and honfels (Ahmadi *et al*., 2007). The compositional variation found in this major pluton, usually range from quartz-dared-tonalite to monzogranite and subvolcanic

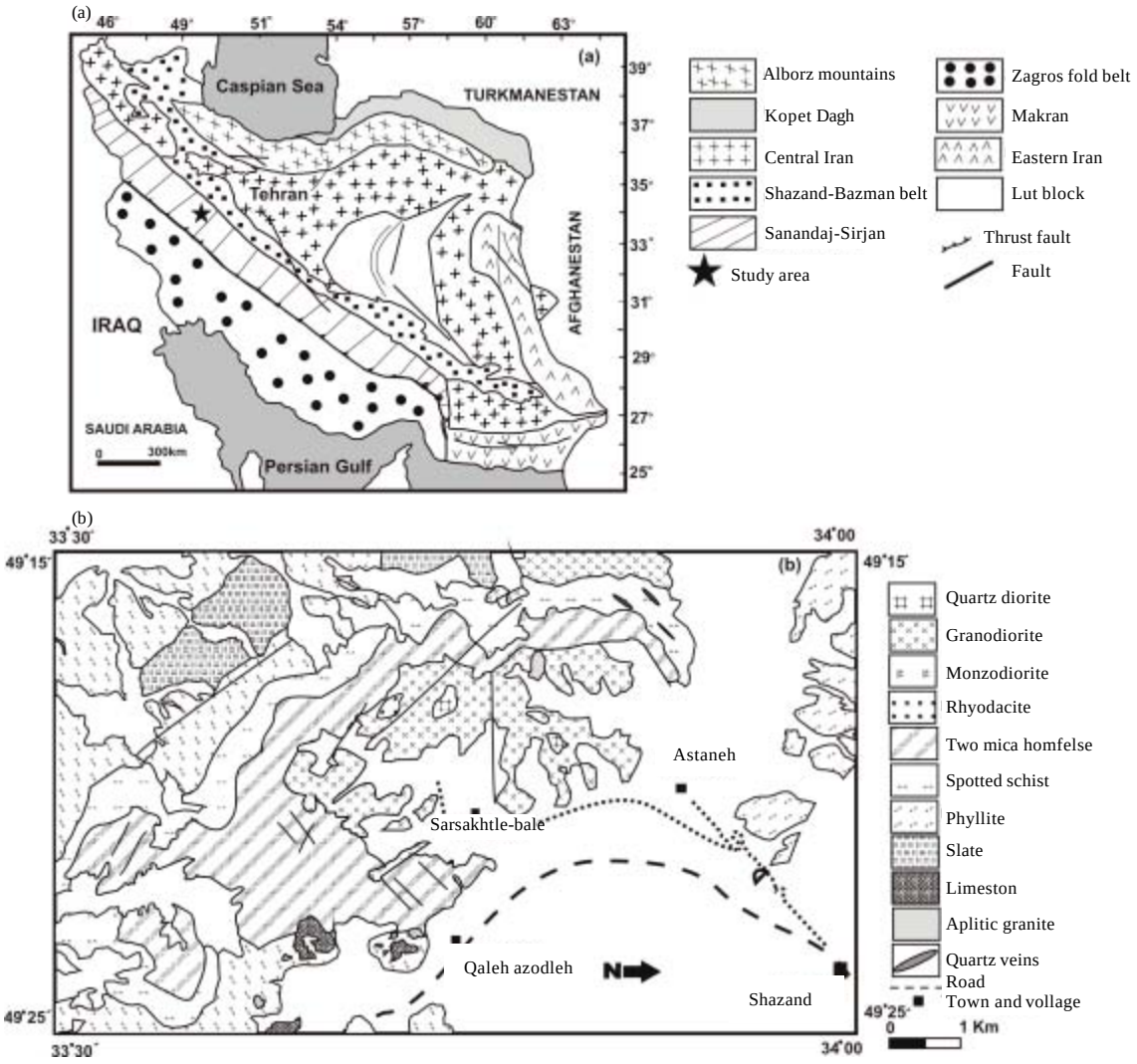

Fig. 1: (a) Geological map of Iran (modified from: Shahabpour, 1994), showing major lithotectonic unites and (b) the Astaneh area, western Iran

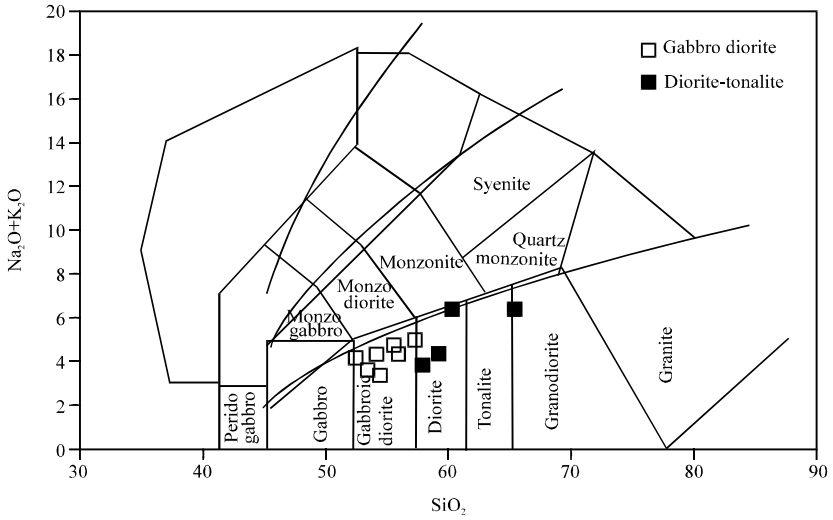

Fig. 2: SiO_2 versus Na_2O+K_2O diagram of the Astaneh granitoids (Middlemost, 1985)

rocks to rhyodacite composition. However, dared and more basic rocks are included large xenoliths in this pluton. A very common feature of Sanandaj-Sirjan Zone granitic type is conspicuous presence of mafic microgranular enclave dispersed, especially in the granodiorites and monzogranites of Astaneh. The granitoids occurring in Astaneh show close similarities with those described elsewhere in the Sanandaj-Sirjan Zone, exceptionally occurrence subvolcanic rocks in Astaneh. In general, mineral assemblage in Astaneh pluton and its related subvolcanic is same to other calc-alkaline granites in Sanadaj-Sirjan Zone.

Petrography and mineral chemistry

Host rock granitoids: The granitoids are variable in grain size, with the principal rock forming minerals ranging from 0.2 to 5.0 mm in diameter. Tonalities and granodiorites are occasionally plagioclase porphyritic whereas granites may have phenocrysts of both plagioclase and quartz. Plagioclase is usually subhedral but can be euhedral, especially when occurring as chadacrysts enclosed by quartz or alkali-feldspar. Quartz is always anhedral and occurs in consertal aggregates. Alkali-feldspar is also anhedral in tonalities and granodiorites, occupying interstices or partially mantling plagioclase. Biotite varies in morphology from anhedral patches, sometimes after amphibole, to subhedral crystals. Amphibole is euhedral to subhedral and occupies interstices between plagioclases. Apatite, zircon and rare sphene are accessory phases.

Enclaves: The enclaves are oval or irregular-shaped masses ranging in size from mm to meters. They appear regularly as inclusions within the granodiorite-monzogranite series. Fine-grained dioritic enclaves are abundant in these rocks. Their size is variable with average lengths of 10-30 cm.

Enclaves range in composition from gabbro dared, dared-tonalite, granodiorite in host granodiorites and dacitic enclaves in rhyodacites (Fig. 2). Granodiorite composition could result from potassic contamination by the host granodiorite.

Gabbro dioritic enclaves: These enclaves are concentrated in the Astaneh granitoid. They range from 5 to 100 cm in diameter, most common size with 20-70 cm (Fig. 3a).

These rocks have fine grain texture (Fig. 3b, c). The main minerals are plagioclase, (30-45 vol.%), usually euhedral, more or less with variable degrees of sericitisation, shows zoning and the first felsic mineral to crystallize. They generally show SiO_2 (51.72-57.5), Al_2O_3 (25.2-29.55), Na_2O (5.23-8.66), CaO (5.4-11.96) and K_2O (<1.0) contents. K-feldspar (<5 vol. %) forms anhedral to subhedral crystals, includes microcline-perthites and a late interstitial phase. They are usually altered to clay minerals. Quartz (<10 vol. %) forms anhedral crystals or aggregates with irregular disordered boundaries, normally occupies the interstices between plagioclas, display recrystallized features with adulatory extinction indicative of incipient solid-state deformation. Amphibole (25-35 vol.%), shows a euhedral prismatic habit, green colour and it is often twinned, associated with biotite and altered to biotite, chlorite, epidote and prehnite. The amphiboles are mainly magnesio-hornblende with a few actinolitic hornblendes on the (Si, P. f.u) Versus ($Mg/Mg + Fe^{2+}$). Amphiboles show ($Ca_B > 1.5$(1.7-1.85), $(Na + K)_A < 0.5$ (0.2-0.3) and thus are calcic amphiboles

Table 2: Representative electron microprobe analysis of pargasitic amphibole in the dacitic enclave and magnesio-hornblende in the mafic microgranular enclave (MME, gabbro dared) from Astaneh pluton, (Number of ions on the basis of 23 oxygen)

	Pargasite in dacitic envlave										Maggnesio-hornblend in gabbro-dioritc enclave											
Sample	AE-1	AE-2	AE-3	AE-4	AE-5	AE-6	AE-7	AE-8	E-9	E-10	11	13	15	17	19	21	23	25	28	30	31	33
SiO_2	42.3	43.4	41.5	41.7	42.1	42.2	42.4	42.5	42.6	41.7	47.7	47.5	47.3	47.6	47.9	47.6	47.3	48.0	47.4	48.1	47.1	47.4
TiO_2	3.3	2.7	3.0	3.3	3.3	3.2	3.1	3.2	3.2	2.7	1.3	1.4	1.4	1.3	1.3	1.3	1.4	1.4	1.4	1.3	1.4	1.5
Pl_2O_3	11.8	11.0	11.4	11.6	11.6	11.6	11.5	11.5	12.0	11.3	6.8	6.6	6.9	6.8	6.7	6.8	7.0	6.4	6.9	6.7	6.9	7.1
FeO^+	10.4	11.8	16.8	11.8	13.4	11.8	10.7	10.9	10.4	16.2	15.2	15.6	15.3	15.1	14.9	15.6	15.0	15.5	15.4	14.8	15.8	15.0
MgO	15.3	14.4	10.4	14.0	12.9	14.0	15.1	14.4	14.4	10.3	12.3	12.3	12.2	12.5	12.5	12.5	12.1	12.6	12.5	12.8	12.4	12.5
MnO	0.1	0.2	0.2	0.2	0.2	0.2	0.2	0.1	0.2	0.3	0.3	0.3	0.3	0.3	0.3	0.3	0.3	0.3	0.3	0.3	0.2	0.3
CaO	11.3	11.0	11.1	11.2	11.3	11.3	11.2	11.2	11.3	11.5	11.1	11.1	11.1	11.1	11.1	11.1	11.4	11.1	10.9	11.2	10.9	10.9
Na_2O	2.4	2.4	2.3	2.7	2.4	2.3	2.5	2.6	2.6	2.1	0.6	0.6	0.7	0.5	0.6	0.6	0.6	0.6	0.8	0.7	0.5	0.6
K_2O	0.6	0.5	0.7	0.6	0.6	0.6	0.6	0.6	0.6	0.8	0.5	0.5	0.5	0.5	0.5	0.6	0.5	0.5	0.6	0.5	0.6	0.6
F	0.0	0.0	0.0	0.0	0.0	0.0	0.0	0.0	0.0	0.0	0.0	0.0	0.0	0.0	0.0	0.0	0.0	0.0	0.0	0.0	0.0	0.0
Cl	0.0	0.0	0.0	0.0	0.0	0.0	0.0	0.0	0.0	0.0	0.0	0.0	0.0	0.0	0.0	0.0	0.0	0.0	0.0	0.0	0.0	0.0
Sum	98.4	97.8	97.7	97.6	98.2	98.0	98.0	97.8	98.0	97.5	96.0	96.2	95.9	95.7	96.0	96.6	95.7	96.3	96.3	96.3	95.9	95.8
T-sites																						
Si	6.2	6.4	6.3	6.2	6.3	6.2	6.2	6.3	6.3	6.3	7.1	7.2	7.1	7.1	7.2	7.1	7.1	7.2	7.1	7.2	7.1	7.1
AlIv	1.8	1.6	1.7	1.8	1.7	1.8	1.8	1.7	1.7	1.7	0.9	0.8	0.9	0.9	0.8	0.9	0.9	0.8	0.9	0.8	0.9	0.9
Al(total)	2.0	1.9	2.0	2.0	2.0	2.0	2.0	2.0	2.1	2.0	1.2	1.2	1.2	1.2	1.2	1.2	1.2	1.1	1.2	1.2	1.2	1.3
M1, 2, 3 Sites																						
AlVI	0.2	0.3	0.3	0.2	0.3	0.3	0.2	0.3	0.3	0.4	0.4	0.3	0.3	0.3	0.3	0.3	0.4	0.3	0.3	0.3	0.3	0.4
Ti	0.4	0.3	0.3	0.4	0.4	0.4	0.3	0.4	0.4	0.3	0.1	0.2	0.2	0.1	0.1	0.2	0.2	0.2	0.2	0.1	0.2	0.2
Fe^{3+}	0.0	0.0	0.0	0.0	0.0	0.0	0.0	0.0	0.0	0.0	0.0	0.0	0.0	0.0	0.0	0.0	0.0	0.0	0.0	0.0	0.0	0.0
Mg	3.3	3.1	2.3	3.1	2.9	3.1	3.3	3.2	3.2	2.3	2.7	2.7	2.7	2.8	2.8	2.8	2.7	2.8	2.8	2.8	2.8	2.8
Mn	0.0	0.1	0.0	0.0	0.0	0.0	0.0	0.0	0.0	0.0	0.0	0.0	0.0	0.0	0.0	0.0	0.0	0.0	0.0	0.0	0.0	0.0
Fe^{2+}	1.0	1.2	2.0	1.3	1.5	1.3	1.1	1.2	1.1	2.0	1.7	1.8	1.7	1.7	1.7	1.7	1.7	1.7	1.7	1.7	1.7	1.7
Ca	0.0	0.0	0.0	0.0	0.0	0.0	0.0	0.0	0.0	0.0	0.0	0.0	0.0	0.0	0.0	0.0	0.0	0.0	0.0	0.0	0.0	0.0
	5.0	5.0	5.0	5.0	5.0	5.0	5.0	5.0	5.0	5.0	5.0	5.0	5.0	5.0	5.0	5.0	5.0	5.0	5.0	5.0	5.0	5.0
M4 site																						
Fe	0.2	0.2	0.2	0.2	0.2	0.2	0.2	0.2	0.1	0.1	0.2	0.2	0.2	0.2	0.2	0.2	0.1	0.2	0.2	0.2	0.3	0.2
Ca	1.8	1.7	1.8	1.8	1.8	1.8	1.8	1.8	1.8	1.9	1.8	1.8	1.8	1.8	1.8	1.8	1.8	1.8	1.7	1.8	1.7	1.7
Na	0.0	0.0	0.0	0.0	0.0	0.0	0.0	0.1	0.1	0.0	0.0	0.0	0.0	0.0	0.0	0.0	0.0	0.0	0.0	0.0	0.0	0.0
	2.0	2.0	2.0	2.0	2.0	2.0	2.0	2.0	2.0	2.0	2.0	2.0	2.0	2.0	2.0	2.0	2.0	2.0	2.0	2.0	2.0	2.0
A site																						
Ca	0.0	0.0	0.0	0.0	0.0	0.0	0.0	0.0	0.0	0.0	0.0	0.0	0.0	0.0	0.0	0.0	0.0	0.0	0.0	0.0	0.0	0.0
Na	0.7	0.7	0.6	0.7	0.7	0.7	0.7	0.7	0.7	0.6	0.1	0.2	0.2	0.1	0.1	0.2	0.2	0.2	0.2	0.2	0.2	0.2
K	0.1	0.1	0.1	0.1	0.1	0.1	0.1	0.1	0.1	0.1	0.1	0.1	0.1	0.1	0.1	0.1	0.1	0.1	0.1	0.1	0.1	0.1
Sum A	0.8	0.7	0.8	0.9	0.8	0.8	0.8	0.8	0.8	0.7	0.2	0.2	0.3	0.2	0.2	0.3	0.3	0.2	0.3	0.2	0.3	0.3
Mg/Mg^+Fe^{2+}	0.8	0.7	0.5	0.7	0.7	0.7	0.8	0.7	0.7	0.5	0.6	0.6	0.6	0.6	0.6	0.6	0.6	0.6	0.6	0.6	0.6	0.6
Fe/Fe^+mg	0.3	0.3	0.5	0.3	0.3	0.3	0.3	0.3	0.3	0.5	0.4	0.4	0.4	0.4	0.4	0.4	0.4	0.4	0.4	0.4	0.4	0.4

occurring to Leake *et al.* (1997) classification, (Fig. 3d, 4a, Table 2) that usually in calc-alkaline granitoids. Biotite, the most abundant mafic mineral (5-15 vol. %) appears in brown flakes. It is frequently associated with amphibole which crystallized before biotite. Most biotite has altered to chlorite, biotite is highly aluminous (Al/Al + Si + Mg + Fe = 0.2-0.22) and ferrous (Fe/Fe + Mg = 0.5-1), thus are biotite occurring to Foster (1960) (Fig. 4c, Table 3). Apatite and the less abundant zircon and allanite occur in all samples. These minerals account for 0.5-1.5% in the modal analysis.

Dioritic enclave: Dioritic enclaves in Astaneh with the dominant size of less than 50 cm are observed in MME. It is supposed that the small enclave within the large MME might be formed by multiple injection of mafic magma (Fig. 5a). Anyway, this more mafic small enclave might be suggesting that magma mixing/mingling was the most possible process to form more mafic small enclaves (Kim *et al.*, 2002).

These rocks have porphyritic and pokilitic texture with plagioclase megacrysts and composed predominantly of plagioclase (40-50 vol. %), amphibole (5-10 vol. %), biotite (15-20 vol. %), alkali feldspar (<5 vol. %), quartz (<10 vol. %). Plagioclase is anhedral to subhedral plates, zoned and altered to sericite, epidote and calcite. Biotite occurs as brown kinking flakes, deformed and altered to chlorite, or broken down to sphene, prehnite, muscovite, opaque and quartz. It is frequently associated with amphibole which crystallized before biotite. Amphibole shows a euhedral prismatic habit, green colour and it is often twinned, associated with biotite and altered to biotite, chlorite, epidote and prehnite. Quartz crystals occur as anhedral to subhedral with adulatory extinction and a late interstitial phase. Alkali feldspar is anhedral to subhedral crystals. Zircon, sphene, apatite are conspicuous accessory minerals. Minor alteration products are sericite, chlorite, epidote, prehnite and calcite.

Table 3: Representative electron microprobe analysis of biotite in dacitic enclave and gabbro dioritic enclave, from Astaneh pluton (Number of ions on the basis of 11 oxygen

	Biotite in dacitic enclave				Biotite in gabbro-dacitic enclave			
Samples	1	2	3	4	5	6	7	8
SiO_2	36.3	35.9	36.1	36.0	36.5	36.5	36.9	36.7
TiO_2	4.1	4.0	3.8	3.7	3.6	3.7	2.5	2.0
Pl_2O_3	13.9	13.9	13.9	13.9	15.3	14.9	15.8	15.9
Cr_2O_3	0.1	0.1	0.1	0.1	0.2	0.2	0.0	0.1
FeOt	22.3	22.3	23.1	22.6	18.5	19.0	19.0	19.7
MnO	0.3	0.2	0.2	0.2	0.2	0.2	0.3	0.3
MgO	9.2	9.3	9.0	9.3	11.0	11.3	10.7	10.4
CaO	0.0	0.0	0.0	0.0	0.0	0.0	0.0	0.0
Na_2O	0.0	0.1	0.1	0.1	0.2	0.2	0.1	0.1
K_2O	9.6	9.7	9.5	9.6	9.1	9.2	9.6	9.4
NiO	0.1	0.1	0.0	0.0	0.0	0.0	0.0	0.0
Total	96.4	95.8	96.1	95.9	94.8	95.4	95.1	94.1
O = Cl, F	0.0	0.0	0.0	0.0	0.0	0.0	0.0	0.0
Total	96.4	95.8	96.1	95.9	94.8	95.4	95.1	95.4
Si	2.9	2.9	2.9	2.9	2.9	2.9	2.9	3.5
Al.IV	1.1	1.1	1.1	1.1	1.1	1.1	1.1	0.5
Al .Vl	0.2	0.2	0.2	0.2	0.3	0.2	0.3	1.2
Ti	0.2	0.2	0.2	0.2	0.2	0.2	0.1	0.1
Cr	0.0	0.0	0.0	0.0	0.0	0.0	0.0	0.0
Fe^{3+}	0.0	0.0	0.0	0.0	0.0	0.0	0.0	0.0
Fe^{2+}	1.4	1.4	1.5	1.5	1.2	1.2	1.2	1.4
Mn	0.0	0.0	0.0	0.0	0.0	0.0	0.0	0.0
Mg	1.1	1.1	1.1	1.1	1.3	1.3	1.2	0.0
Ni	0.0	0.0	0.0	0.0	0.0	0.0	0.0	0.0
Oct	3.0	3.0	3.0	3.0	3.0	3.0	3.0	2.9
Ca	0.0	0.0	0.0	0.0	0.0	0.0	0.0	0.0
Na	0.0	0.0	0.0	0.0	0.0	0.0	0.0	0.0
K	1.0	1.0	1.0	1.0	0.9	0.9	1.0	1.1
Tota	3.9	4.0	3.9	4.0	3.9	3.9	3.9	4.0
XMg	0.4	0.4	0.4	0.4	0.5	0.5	0.5	0.0
FeO	22.3	22.3	23.1	22.6	18.5	19.0	19.0	19.7
Fe_2O_3	0.0	0.0	0.0	0.0	0.0	0.0	0.0	0.0
FeOtot	22.3	22.3	23.1	22.6	18.5	19.0	19.0	19.7
$Fe/Fe^{+}Mg$	0.6	0.6	0.6	0.6	0.5	0.5	0.5	1.0
R^{3+}	0.4	0.4	0.4	0.4	0.5	0.4	0.5	1.4
R^{2+}	1.5	1.5	1.5	1.5	1.2	1.2	1.2	1.4
$Altot/Ca^{+}Na^{+}K$	1.3	1.3	1.3	1.3	1.5	1.5	1.2	1.5

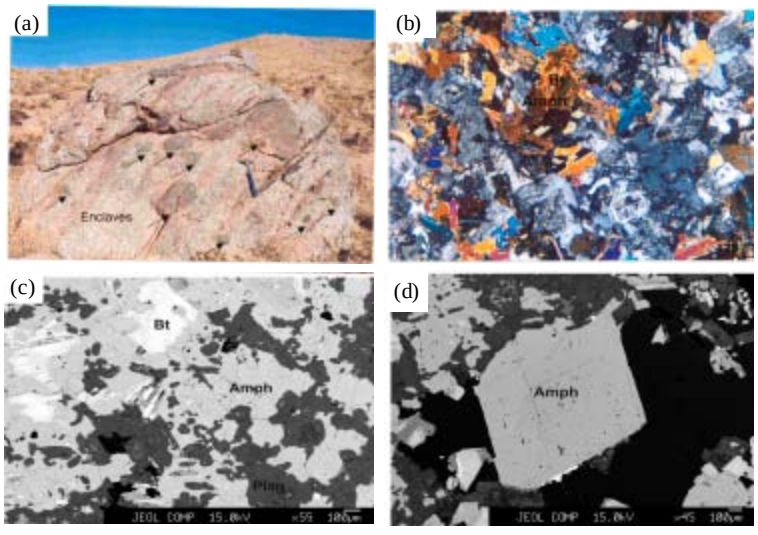

Fig. 3: (a) MME in the Astaneh granitoids, (b) fine grain texture micro gabbro dared, backscattered electron image (BSE) to representative samples, (c) Bt, Amph and Plag in MME and (d) Euhedral Magnesio-hornblende in mafic Microgranular enclave. Bt = biotite; Amph = amphibole; Mineral abbreviations are according to Kretz (1983)

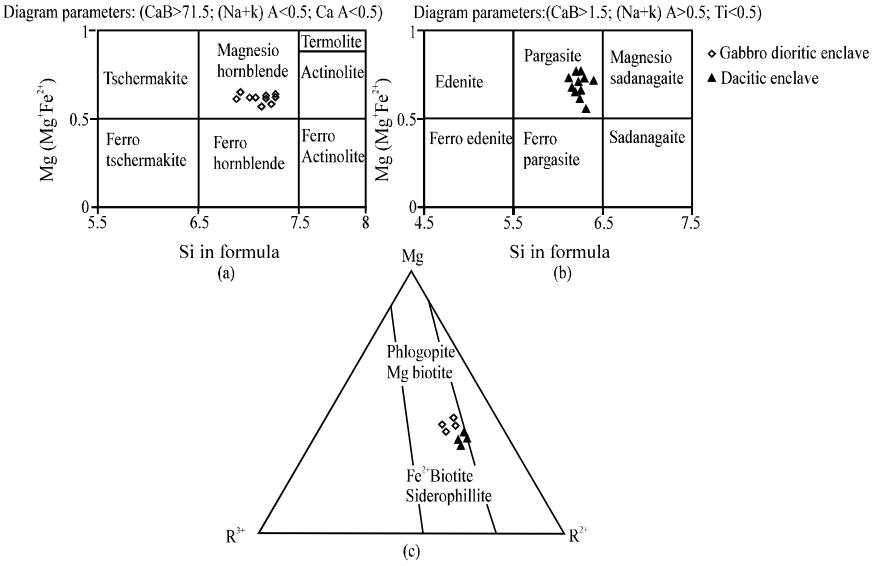

Fig. 4: Classification of amphibole and biotite in gabbro dioritic and dacitic enclaves in Astaneh pluton according to Leake *et al.* (1997) and Foster (1960), respectively. (a) showing crystallization of magnesio-hornblende in gabbro dioritic dioritic, (b) pargasite in dacitic enclave and (c): Plots of (a) R^{2+} (Fe^{2+} +Mn)-Mg-R^{3+} (Fe^{3+}+Ti +Al ^{VI}) of Foster (1960)

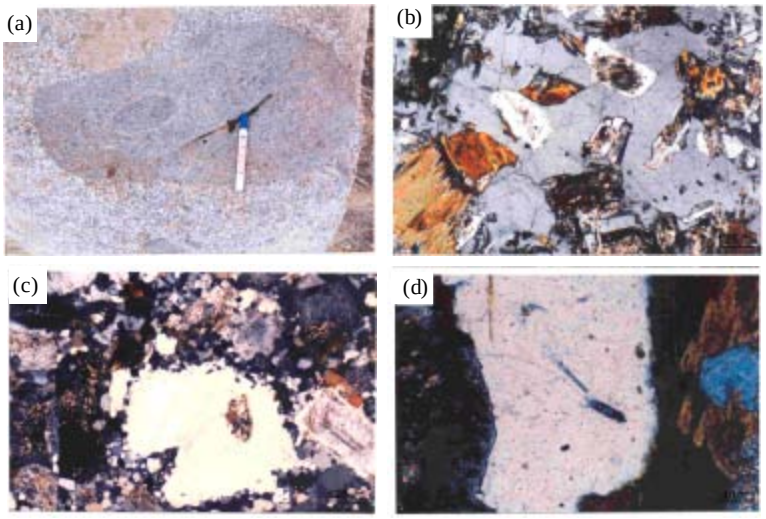

Fig. 5: (a) Double enclave (enclave within enclave) in Astaneh pluton, (b) poikilitic texture in dioritic enclave, (c) quartz ocelli in dioritic enclave and (d) acicular apatite in Alkali feldspar

The crystal shapes of K-feldspar, simple twinning and its zoned euhedral plagioclase inclusions found in the dioritic-tonalitic enclaves suggest that they have an igneous origin (Vernon and Paterson, 2002). Their mineralogy and texture show that have a multistage crystallization (Castro *et al.*, 1991). These enclaves have a co-magmatic composition with their host. Accessory minerals include opaque phases, titanite and apatite. Chlorite, epidote and sericite occur as alteration phases. Dioritic enclave (e.g., E-29 and E-28) are essentially composed of calcic amphibole (magnesio-hornblende) and andesine plagioclase (An = 35-40) and subordinate biotite. Needle-like apatite preferentially occurs in plagioclase and quartz. Secondary mineral usually fill cleavages and intergranular boundaries.

Poikilitic texture which is commonly observed in the quartz dioritic enclave (Fig. 5b), large (4-5 mm in size) quartz or alkali feldspar phenocrysts including small

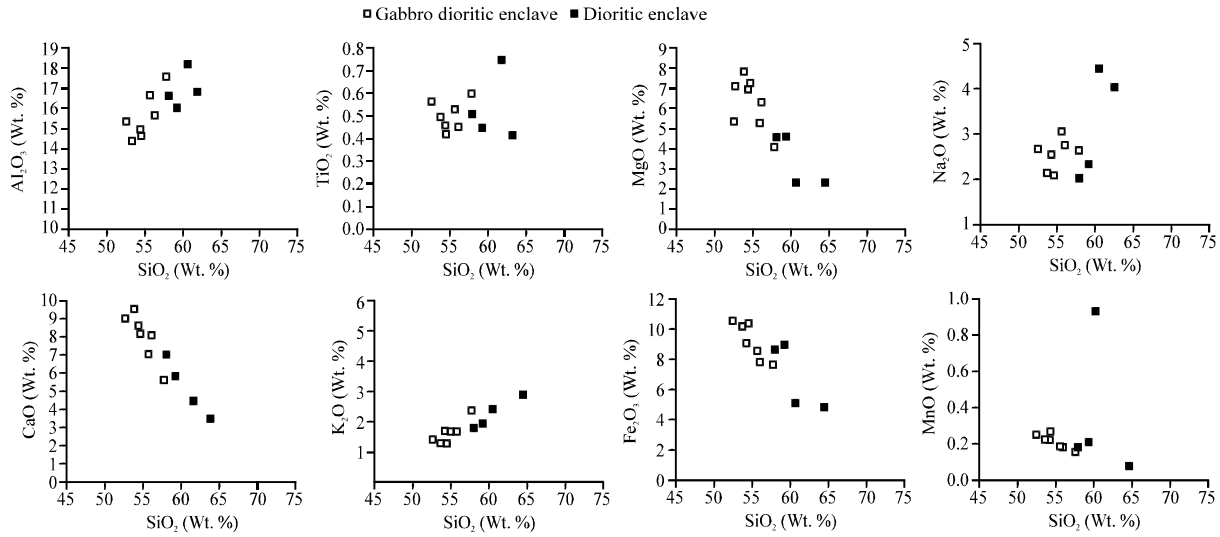

Fig. 6: Harker variation diagrams of selected major element oxides

(0.1-0.5 mm in size) plagioclase, amphibole, biotite and apatite. This texture probably result from: (1) the growth of quartz and alkali feldspar phenocrysts during the crystallization, capturing pre-existing plagioclase, amphibole, biotite and so in common crystallization history and (2) late stage crystallization of felsic melt after the crystallization of abundant quench-generated plagioclase, amphibole, biotite and apatite in relation to magma mixing (Hibbard, 1991). If the poikilitic texture had been formed by the former case, the included minerals would have arranged after the crystal growth face of the quartz and alkali feldspar phenocrysts during the crystallization, however most of the included minerals orient randomly, therefore it is considered that the texture might be formed by the later case and partially dissolved portions are observed occasionally in the boundary between the phenocrysts and the included minerals, therefore by mafic magma injection into felsic magma, quartz and alkali feldspar phenocrysts were corroded and plagioclase, amphibole, biotite and apatite from mafic magma were supercooled during the crystallization of these phenocrysts in granitic magma.

The ocellar and ovoid textures (Fig. 5c) are found in MME. The ocellar texture is mantling quartz and alkali feldspar ovoid phenocrysts (1-2 mm in size) with fine-grained mineral association of amphibole±biotite±plagioclase or a single mineral. Some ovoid occur without mantling. The ovoid grains of quartz and alkali feldspar were formed by the dissolution of pre-existing crystals owing to high temperature environment by the inflow of phenocrysts from the granite into the MME (Hibbard, 1991). This suggests that at the time of magma mafic injected, there were already existing alkali feldspar and quartz grains in the granitic system because compositions of MME could not crystallize quartz phenocryst in the early stage of crystallization (Johannes and Holtz, 1996).

MME have acicular crystals of apatite (Fig. 5d). Rapid growth of apatite in a quenched magmas results in acicular shape, rather than stubby prismatic or prismatic one (Reid *et al*., 1983). Acicular apatite in granitic rocks has also been identified as a mixing/mingling texture (Didier, 1987).

Dacitic enclaves: In these rocks, Quartz, plagioclase and biotite occurs as phenocrysts in a seriate texture. Normal alteration is to aggregates of chlorite, opaque minerals and epidote. These rocks contains numerous phenocrysts of pargasitic amphibole to $Ca_B > 1.5(1.71-1.77)$, $(Na + K)_A > 0.5(0.55-0.7)$ (Fig. 4b) and plagioclase in fine grain matrix of biotite and plagioclase.

The absence of clinopyroxene in gabbro dioritic, dioritic and dacitic enclave may result from rapid cooling of the mafic magma down to the stability field of amphibole and plagioclase, inhibiting nucleation of higher-temperature phases (Blundy and Spark, 1992).

Geochemical characteristics of the enclaves: Representative whole- rock major and trace elements compositions of Astaneh enclaves and average of host rocks are reported in Table 1. Major elements variations are shown in Harker diagrams in Fig. 6. The investigated rocks show compositional variations, especially in their silica content. The samples exhibit a range in SiO_2 content from approximately 52 to 65 wt%. Fe_2O_3, MgO, CaO, TiO_2 and MnO abundances decrease with increasing SiO_2, whereas K_2O, Al_2O_3 and Na_2O increase.

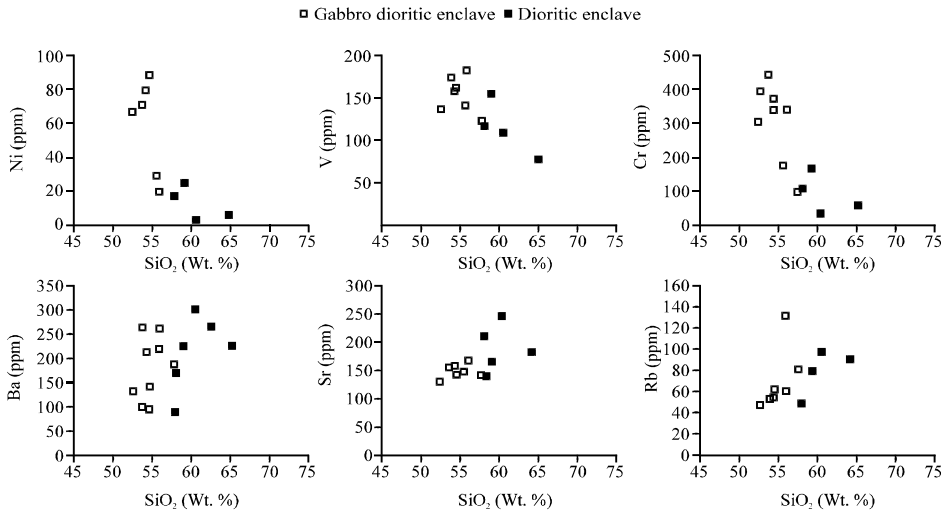

Fig. 7: Harker variation diagrams of selected trace element versus SiO_2 content

The highest MgO content in the plot is for gabbroic enclaves which have high modal proportions of Ca-amphibole.

The highest MgO content in the plot is for gabbroic enclaves which have high modal proportions of Ca-amphibole.

The trace elements behave in a similar way when plotted versus increasing SiO_2 content (Fig. 7), decreasing trends for V, Cr, Ni, Co and increasing trends for Rb and Sr. Transition elements (Ni, Cr, Co, V) decrease with increasing SiO_2 content, in agreement with their incorporation into early-crystallized ferro-magnesian silicates.

DISCUSSION

The Astaneh enclaves have gabbro dared to dioritic compositions. Enclaves with a magmatic texture are found in almost all the granitoid plutons. Vernon *et al.* (1988) have emphasized that rounded to ellipsoidal shapes to enclaves are strong indication of magma mingling and flow.

In felsic plutons, the volume of more mafic magma is much less than that of the more felsic magma, so that quenching and pillowing of the more mafic magma occurs; i.e., the magmas commonly mingling, rather than mixing (Kouchi and Sunagawa, 1983; Vernon, 1983, 1984; Sparks and Marshall, 1986).

These enclaves are microgranular in texture and rich in mafic minerals and, in descriptive terms, appear to be mafic microgranular enclaves (Didier and Barbarin, 1991) which are generally accepted to represent products of incomplete mixing (mingling) between mafic (enclave) and felsic (host granitoids) magmas (Eberz and Nicholls, 1988; Dorais *et al*., 1990; Didier and Barbarin, 1991). Indeed very fine-grained equigranular texture of MME (Fig. 3b) reflects that mafic magma was in near liquids state when it was injected into granitic magma.

The characteristic petrographic features of MME are the presence of: (i) acicular apatites (resulting from rapid growth in an internally quenching mixing system); (ii) poikilitic feldspars (containing mafic mineral inclusions); and (iii) quartz ocelli (resulting from the undercooling-generated mafic crystals of a mafic system around a nucleus of early-formed quartz minerals of felsic system), which are widely accepted as evidence of mixing/ mingling (Eberz and Nicholls, 1988; Hibbard, 1991; Vernon, 1991).

Gabbro- dioritic, dioritic and dacitic enclaves have I-type mineral assemblages that are broadly similar to those in the host granitoids except for the greater abundance of mafic minerals, such as amphibole.

Their chemistry contains the lowest values of SiO_2 and the highest CaO and MgO for the enclaves. This similarity in mineralogy between enclaves and host rock is explained by Van Der Laan and Wyllie (1993) from a series of acid-basic experiments. According to authors, if mafic minerals are in equilibrium with the melt in the mafic domain and if the melts in both are mutually equilibrated, then the minerals in enclaves should also be in equilibrium with the melt in the granitic domain and therefore they should be similar to the mafic minerals simultaneously or subsequently precipitated from the granitic host magma with decreasing temperature. Moreover the same mineral assemblage would support thermal equilibrium states in granite and enclaves (Pitcher, 1991).

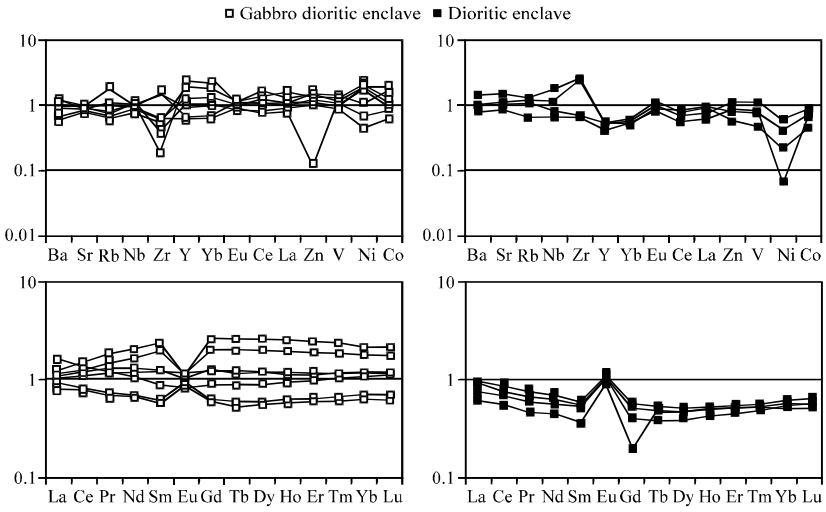

Fig. 8: REE and trace elements composition of enclaves normalised against their host granitoids

This together with the occurrence of enclave within enclave (Fig. 5a) implies than mingling between these enclaves and host granodiorites.

The elevated Sr values displayed in these rocks may be attributed to the influence of the mafic magma (Fig. 8). We consider that the more Sr enrichmentin enclaves than host grandiorities ascribed toxenocrysts of oscillatory-zoned, calcic rich, plagioclase feldspars which are a known repository of Sr (Poli and Tommasini, 1991) and which were introduced by the injection of the mafic magma. Besides plagioclase, Sr may have also have been contributed through the presence of the calcic amphiboles, sphene and apatite.

According to Nardi and Lima (2000), the least hybridized enclaves are those with SiO_2 lower than 55 wt.% and MgO higher than 4.5 wt.%, the slightly hybridized are those with SiO_2 close to 56 wt.% , the moderately hybridized are those with SiO_2 close to 58 wt.% and finally, the strongly hybridized enclaves are those with SiO_2 varying from 60-65 wt.% . In Astaneh pluton, the least and slightly enclaves are restricted to the gabbroic and dioritic enclaves. In order to illustrate the geochemical effects of hybridism in the enclaves of the Astaneh granitoids, their major and trace components were normalised against the host rock average (Fig. 8). Rare earth element patterns of gabbro dared and dioritic enclaves normalised against the host rock average reproduce the flat shape except Eu contents controlled by added feldspar, as indicated by pronounced positive and negative Eu anomalies. So, the increase of Nb in enclaves of I-type granites can be interpreted as an evidence of preferential Nb diffusion to mafic microgranular enclaves (Green, 1995).

CONCLUSIONS

The enclaves in Astaneh granitoid are classified into microgabbrodiorite, microdiorite and less than microgranodiorite. Granodiorite composition could result from potassic contamination by the host granodiorite. These enclaves demonstrate that the clearest evidence for an origin through mingling processes is provided by field and petrographic features, such as chilled margins against the host granite, the presence of ocelli quartz and feldspar as megacrysts in dioritic enclaves, poikilitic texture, acicular apatites and double enclaves. In addition, geochemical normalised diagrams against average granite showed the dominant process in forming of enclaves was magma mingling.

ACKNOWLEDGMENTS

This study is part of the Ph.D Thesis by Z.T. Dr. Mohammad Ali Mackizadeh at University of Isfahan and Mehraj Aghazadeh at University of Tarbiat Moddares is thanked. The geochemical study was carried out in the University of Huelva (Spain) during a study leave of Z.T.

REFERENCES

Ahmadi, K.A., D. Esmaeily, M.V. Valizadeh and H.R. Bonab, 2007. Petrology and geochemistry of the granitoid complex of Boroujerd, Sanandaj-Sirjan Zone, Western Iran. J. Asian Earth Sci., 29: 859-877.

Baharifar, A., H. Moinevaziri, H. Bellon and A. Piqué, 2004. The crystalline complexes of Hamadan (Sanandaj-Sirjan zone, western Iran): Metasedimentary Mesozoic sequences affected by late cretaceous tectono-metamorphic and plutonic events. C. R. Geosci., 336: 1443-1452.

Barbarin, B. and J. Didier, 1991. Conclusions: Enclaves and Granite Petrology. In: Enclaves and Granite Petrology, Didier, J. and B. Barbarin (Eds.). Elsevier, Amsterdam, ISBN: 0-444-89145-5, pp: 545-549.

Barbarin, B. and J. Didier, 1992. Genesis and evolution of mafic microgranular enclaves through various types of interaction between coexisting felsic and mafic magmas. Trans. R. Soc. Edinb., 83: 145-153.

Blundy, J.D. and R.S.J. Sparks, 1992. Petrogenesis of mafic inclusions in granitic of the Adamello massif, Italy. J. Petrol., 33: 1039-1104.

Castro, A., J.D. Rosa and W.E. Stephens, 1990. Magma mixing in the subvolcanic environment: Petrology of the Gerena interaction zone near Seville, Spain. Contrib. Miner. Petrol., 105: 9-26.

Castro, A., I. Moreno-Ventas and J.D. De La Rosa, 1991. Multistage crystallization of tonalitic enclaves in granitoid rocks. Implications in magma mixing. Geol. Rund., 80: 109-120.

Cotton, J.A.M., M. Le Dez Bau, R.C.P. Caroff and S. Maury *et al*., 1995. Origin of anomalous rare earth element and yttrium enrichment in subaerially exposed basalts: Evidence from France Polynesia. Chem. Geol., 119: 115-138.

Dahlquist, J.A., 2002. Mafic microgranular enclaves: Early segregation from metaluminous magma (Sierra de Chepes), Pampean Ranges, NW Argentina. J. South Am. Earth Sci., 15: 643-655.

Didier, J., 1987. Contribution of Enclave Studies to the Understanding of Origin and Evolution of Granitic Magmas. In: Enclaves and Granite Petrology, Didier, J. and B. Barbarin (Eds.). Elsevier, Amsterdam, ISBN: 0-444-89145-5, pp: 83-94.

Didier, J. and B. Barbarin, 1991. Enclaves and Granite Petrology. 1st Edn. Elsevier, Amsterdam, ISBN: 0-444-89145-5, pp: 601.

Dodge F.C.W. and R.W. Kistler, 1990. Some additional observations on inclusions in the granitic rocks of the Sierra Nevada. J. Geoph. Res., 95: 841-848.

Dorais, J.M., J.A. Whitney and M.F. Roden, 1990. Origin of mafic enclaves in the Dinkey Creek Pluton, Central Sierra Nevada Batholith, California. J. Petrol., 34: 853-881.

Eberz, G.W. and I.A. Nicholls, 1988. Microgranitoids enclave from the Swift Creek Pluton SE-Australia: Textural and physical constraints on the nature of magma mingling process in the plutonic environments. Geol. Rund., 77: 713-736.

Fershtater, G.B. and N.S. Borodina, 1991. Enclaves in the Hercynian Granitoids of the Urals Mountains, USSR. In: Enclaves and Granite Petrology, Didier, J. and B. Barbarin, (Eds.). Elsevier, Amsterdam, ISBN: 0-444-89145-5, pp: 83-94.

Foster, M.D., 1960. Interpretation of the composition of trioctahedral. US. Geol. Surv. Prof. Pap., 354-B: 1-49.

Green, T.H., 1995. Significance of Nb/Ta as an indicator of geochemical processes in the crust-mantle system. Chem. Geol., 120: 347-359.

Hibbard, M.J., 1991. Textural Anatomy of Twelve Magma-Mixed Granitic Systems. In: Enclaves and Granite Petrology. Didier, J. and B. Barbarin (Eds.). Elsevier, Amesterdam (Dev Petrol 13), ISBN 0-444-89145-5, pp: 431-444.

Johannes, W. and F. Holtz, 1996. Petrogenesis and Experimental Petrology of Granitic Rocks. 1st Edn. Springer, Berlin, ISBN: 3-540-60416-2, pp: 1-335.

Kim, J.S., K.C. Shin and J.D. Lee, 2002. Petrographical study on the Yucheon granite and its enclaves. Geosci. J., 6: 289-302.

Kouchi, A. and I. Sunagawa, 1983. Mixing basaltic and andesitic magmas by forced convection. Nature, 304: 527-528.

Kretz, R., 1983. Symbols for rock-forming minerals. Am. Min., 68: 277-279.

Leake, B.E., A.R. Woolley, C.E.S. Arps, W.D. Birch and M.C. Gilbert *et al*., 1997. Nomenclature of amphiboles: Report of the subcommittee on amphiboles of the International Mineralogical Association, Commission on new minerals and mineral names. Can. Mineral., 35: 219-246.

Maas, R., I.A. Nicholls and C. Legg, 1997. Igneous and metamorphic enclaves in the S-type Deddick Granodiorite, Lachlan Fold Belt, SE Australia: Petrographic, geochemical and Nd-Srisotopic evidence for crustal melting and magma mixing. J. Petrol., 38: 815-841.

Middlemost, E.A.K., 1985. Magmas and Magmatic Rocks. 1st Edn. An Introduction to Igneous Petrology, Longman Groupuk, London, ISBN: 0582300800, pp: 73-87.

Nardi, L.V.S. and E.F. Lima, 2000. Hybridisation of mafic microgranular enclaves in Lavras granite Complex, southern Brazil. J. South Am. Earth Sci., 13: 67-78.

Pitcher, W.S., 1991. Synplutonic Dykes and Mafic Enclaves. In: Enclaves and Granite Petrology, Didier, J. and B. Barbarin (Eds.). Elsevier, Amsterdam, ISBN: 0-444-89145-5, pp: 383-392.

Poli, G.E. and S. Tommasini, 1991. Model for the origin and significance of microgranular enclaves in calc-alkaline granitoids. J. Petrol., 32: 657-666.

Reid, J.R., O.C. Evans and D.G. Fates, 1983. Magma mixing in granitic rocks of the central Sierra Nevada, California. Earth Planet Sci. Lett., 66: 243-261.

Shahabpour, J., 1994. Post-mineralization breccia dike from the SarCheshmeh porphyry copper porphyry system, Kerman, Iran. Expl. Min. Geol., 3: 39-43.

Sinha, K.K., Nautiyal-Kuldeep, P.K. Sharma and R.K. Gupta, 2001. Petrochemical evidences of magma mingling and mixing in Bundelkhand Massif, Rajghat, Uttar Pradesh, Gondwana. Geol. Mag., 13: 1-11.

Sparks, R.S.J. and L.A. Marshall, 1986. Thermal and mechanical constraints on mixing between mafic and silicic magmas. J. Volcanol. Geotherm. Res., 29: 99-124.

Tobisch, O.T., B.A. McNulty and R.H. Vernon, 1997. Microgranitoid enclave swarms in granitic plutons, Central Sierra Nevada, California. Lithos, 40: 321-339.

Van der Laan, S.R. and P.J. Wyllie, 1993. Experimental interaction of granitic and basaltic magmas and implications for mafic enclaves. J. Petrol., 34: 491-517.

Vernon, R.H., 1983. Restite, xenoliths and microgranitoid enclaves in granites (Clarke Memorial Lecture). J. Proc.. R. Soc. New South Wales, 116: 77-103.

Vernon, R.H., 1984. Microgranitoids enclaves: Globules of hybrid magma quenched in a plutonic environment. Nature, 309: 438-439.Vernon, R.H., M.A. Etheridge and V.J. Wall, 1988. Shape and microstructure of microgranitoids enclaves: Indicators of magma mingling and flow. Lithos, 22: 1-11.

Vernon, R.H., 1990. Crystallization and hybridism in microgranitoid enclave magmas: Microstructural evidence. J. Geophs. Res., 95: 849-859.

Vernon, R.H., 1991. Interpretation of Microstructures of Microgranitoid Enclaves. In: Enclaves and Granite Petrology 13, Didier, J. and B. Barbarin (Eds.). Elsevier, Amsterdam, ISBN: 0-444-89145-5, pp: 277-292.

Vernon, R.H. and S.R. Paterson, 2002. Igneous origin of K-feldspar megacrysts in deformed granite of the papoose flat pluton Visual Geosci., 7: 1-28.

Wiebe, R.A., D. Smith, M. Sturn, E.M. King and M.S. Seckler, 1997. Enclaves in the Cadillac mountain granite (Coastal Maine): Samples of hybrid magma from the base of the chamber. J. Petrol., 38: 393-426.